European Journal of Pharmaceutical Sciences 191 (2023) 106611

Contents lists available at ScienceDirect

European Journal of Pharmaceutical Sciences

journal homepage: www.elsevier.com/locate/ejps

Image-based simultaneous particle size distribution and concentration measurement of powder blend components with deep learning and machine vision

Máté Ficzere, Orsolya Péterfi, Attila Farkas, Zsombor Kristóf Nagy *, Dorián László Galata

Department of Organic Chemistry and Technology, Faculty of Chemical Technology and Biotechnology, Budapest University of Technology and Economics, Műegyetem rkp 3., Budapest H 1111, Hungary

ARTICLE INFO

Keywords:
Powder blending
Machine vision
Deep learning
YOLOv5
PAT
API concentration measurement
Particle size distribution

ABSTRACT

This work presents a system, where deep learning was used on images captured with a digital camera to simultaneously determine the API concentration and the particle size distribution (PSD) of two components of a powder blend. The blend consisted of acetylsalicylic acid (ASA) and calcium hydrogen phosphate (CHP), and the predicted API concentration was found corresponding with the HPLC measurements. The PSDs determined with the method corresponded with those measured with laser diffraction particle size analysis. This novel method provides fast and simple measurements and could be suitable for detecting segregation in the powder. By examining the powders discharged from a batch blender, the API concentrations at the top and bottom of the container could be measured, yielding information about the adequacy of the blending and improving the quality control of the manufacturing process.

1. Introduction

Powder blending is a process that is part of practically all pharmaceutical manufacturing lines and is critical for the quality of the final drug product. The purpose of this operation is to prepare uniform blends that can be used during the later manufacturing steps (Sánchez-Paternina et al., 2019). It is essential to verify that the mixing of the active pharmaceutical ingredient (API) and the excipients has been done properly, as differences in the concentration of the blend can affect important quality attributes of the final product, for example, the content uniformity of tablets (Galata et al., 2021a).

Content uniformity is influenced by different factors such as the design and the operation conditions of the blender, the flow properties of the API and the segregation of the powder blend. The first step in guaranteeing content uniformity is ensuring powder blend uniformity, because the API distribution directly influences the dose of the drug that the patient consumes. Therefore, to prevent under- or overdosing patients, in-process testing of the produced powder blends is required by the Good Manufacturing Practice (GMP) (Sierra-Vega et al., 2019). The testing is conducted by inserting sample thieves into the blender to gather the material. However, this disrupts the material flow around the sampler and could influence the composition of the extracted substance (Berman et al., 1996). Two draft guidelines were issued by the United States Food and Drug Administration assessing the problems of sampling pharmaceutical powder blends, of which the first was withdrawn and the second never got approval (Esbensen et al., 2016; Garcia et al., 2015). Following the Process Analytical Technology paradigm (Food and Administration, 2004), the evaluation of blended powders has shifted to real-time monitoring utilizing various sensors (Romañach, 2015).

Currently, the adequacy of powder mixing is usually tested with high-performance liquid chromatography (HPLC) analysis of the taken powder samples, resulting in costly and time consuming tests (Romañach, 2015). In addition, after solving the solid sample to inject it into the column, this method does not provide information about the particle size distribution of the sample. The shape and size of particles can influence the processability and quality attributes of powders, including dissolution and drug release rate, flow properties and susceptibility to segregation (Shekunov et al., 2007). A change in a component's particle size could induce segregation in the subsequent manufacturing steps, therefore it could be advantageous to monitor it after the blending process (Jakubowska and Ciepluch, 2021).

Near infrared (NIR) and Raman spectroscopy are both capable methods for the non-invasive monitoring of the powder blending

* Corresponding author.
E-mail address: zsknagy@oct.bme.hu (Z.K. Nagy).

https://doi.org/10.1016/j.ejps.2023.106611
Received 11 April 2023; Received in revised form 21 August 2023; Accepted 14 October 2023
Available online 15 October 2023

process, however NIR spectroscopy is more well-established (Nagy et al., 2019). Both these methods can be used for real-time analysis, resulting in more representative sampling and shorter batch times (Cullen et al., 2015). Raman (Lee et al., 2012) and NIR spectroscopy (Razuc et al., 2019) have both been used for blend uniformity assessment and end-point detection, although these methods have a higher investment cost and the analysis of the collected spectra requires specific chemometric expertise.

Digital cameras are more affordable sensors that are capable of recording sharp images of particles of powders, enabling the measurement of their shape and size, and the determination of API concentration in the case of coloured APIs. They are considered to be capable of becoming robust PAT tools for many manufacturing steps, mainly in the case of granulation and crystallization, but also during blending as well. (Galata et al., 2021b). Adressing sample representativeness is just as a key factor during image analysis as with any other measurement method. This can be achieved by using multiple cameras with different focal planes or with more frequent measurements (Muthudoss et al., 2022; Saravanan et al., 2021). Madarász et al. were the first to implement feedback control for a twin-screw wet granulation system (TSWG) based on the analysis of in-line acquired images. The real-time gathered PSD data was used to manage the particle size of the granules by altering the speed of the used peristaltic pump dispensing the granulation liquid via an algorithm, resulting in a Process Analytically Controlled Technology (PACT) (Madarász et al., 2018). Gosselin et al. (Gosselin et al., 2017) utilized an RGB camera, light induced fluorescence (LIF) and NIR spectroscopy together to measure the concentration of different coloured components of vitamin blends inside a tablet press feed frame. They used these analytical tools to detect the transitions between the blends. The results showed that the RGB camera is capable of monitoring the flow of the coloured components during transitions. However, there are no cases where images acquired by digital cameras were used to determine the API concentration of a non-coloured powder blend.

Thanks to the recently occurring major improvements in the field of convolutional neural networks (CNN), the accuracy and speed of their inference have greatly increased, making real-time object recognition achievable (Ficzere et al., 2022). Several methods have been developed to evalute the accuracy of different object detection algorithms. Intersection over union (IOU) measures the area of overlap between a true and a predicted bounding box divided by the union of their area. We can determine whether a detection is correct or incorrect by comparing the IOU with a predetermined threshold, and it can be used to calculate precision (P) and recall (R) (Rezatofighi et al., 2019). Precision can be obtained by deviding the number of true positive (TP) detections with the number of all detections and it can show that the developed model only identifies desired objects. Recall demonstrates the ability of fiding all of the relevant objects and is calculated by deviding the number of TPs with all ground truths. For an object detection algorithm to be considered good, both its P and R value should be high. The accuracy of object detectors across all classes in a particular database is evaluated using the mean average precision (mAP) metric. As its name suggests, it is the mean of the average precision calculated for all classes, which can be determined by the area under the precision-recall curve (Padilla et al., 2020). Loss functions are used for measuring the accuracy of the classification, by calculating the errors between the true and predicted labels, which are then combined into the loss value that is utilized for the training of the network. There are numerous types of losses, but the most important ones are the cross-entropy loss, which is based on the probabilities of the classification and the bounding box regression or box loss which is calculated using the differences of the coordinates of the bounding boxes (Li et al., 2020).

There are several applications of CNNs in the fields of powder technology and pharmaceutical sciences (Ficzere et al., 2022; Hirschberg et al., 2020; Iwata et al., 2022; Ma et al., 2020; Sachs et al., 2023). Sachs et al. used a deterministic algorithm and a deep neural network for particle size classification of suspended tracer particles. They found that the neural network has a higher precision of 99.3 % and does not require a change in the existing measurement setup (Sachs et al., 2023).

The examination of the existing literature revealed that the particles could be recognized and circumscribed using neural networks, however no study has been reported on using CNN to recognise the different components of a powder mix simultaneously. Therefore, the purpose of this study is to develop a system, which can monitor both the API concentration and the per component PSD of powder blends at the same time. For the recognition of the particles, we aim to utilize the recently released YOLOv5 object detection algorithm. The proposed system offers a more thorough inspection of the discharged powder mixes, enabling a better understanding of the pharmaceutical blending process.

2. Materials and methods

2.1. Materials

Acetylsalicylic acid (ASA) was obtained from Molar Chemicals (Halásztelek, Hungary). Anhydrous calcium hydrogen phosphate (CHP) was acquired from JRS Pharma (Rosenberg, Germany). Fig 1 presents the microscopic images of the used materials.

2.2. Methods

2.2.1. Preparation of powder blends

The powder blends were prepared by mixing together ASA and CHP in small plastic containers. These each contained 20 g of powder and were homogenized using hand motion for 5 min each. The API concentration of the blends was 0–2–4–6–8–10 % for the calibration experiments and 3–5–6–7 % for validation.

2.2.2. Real-time imaging

The powders were loaded into a LABORETTE 24 vibratory feeder (Fritsch GmbH, Idar-Oberstein, Germany) equipped with a V-shaped chute operated at 5 % vibrational amplitude intensity. The powder leaving the feeder fell onto moving transparent plastic sheets, which were placed on a conveyor belt (Brabender Technologie, Duisburg, Germany) operated at 16,6 mm/s. Directly after the particles left the conveyor belt, they were illuminated from below with a 12 W LED panel (Mentavill, Székesfehérvár, Hungary), which provided evenly

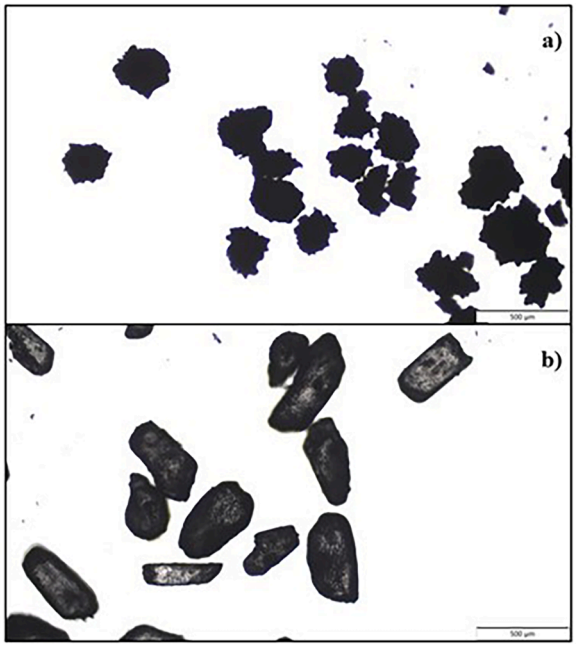

Fig. 1. Light microscopic images of a) $CaHPO_4$ b) ASA.

distributed lightning. To prevent the sheets from falling over, they were underset using supports. A 12-megapixel, area scan Basler acA4112-30uc RGB camera (Basler, Ahrensburg, Germany) equipped with a Mitutoyo 375-036-2 objective (Mitutoyo Corporation, Kawasaki, Japan) and a telescope was mounted directly above the illuminated area for image acquisition. The exposure time was set to 3 ms. 2 images were obtained each second with a size of 2000 by 3000 pixels. The system was operated for 10 min for each concentration level. During this time, approximately 5 g of powder containing 150,000 particles passed under the camera for each level. The setup can be observed in *Fig. 2*.

2.2.3. Training of the YOLOv5 algorithm for particle recognition

The yolov5s6 version of the YOLOv5 model (correction of reference) was trained in Google Colab. Separate YOLOv5 models were trained for the detection of ASA and CHP. To acquire images, the measurement setup was operated using pure ASA, pure CHP and a 50–50 m/m% blend. The taken images were manually annotated with bounding boxes for the different particles and then were split into datasets for training and validation. Fig. 3 presents a flow chart showing the different workflows in order.

The training images contained 2751 ASA and 2851 CHP particles, while the ones used for validation had 1104 ASA and 1054 CHP particles. The input image size was set to 2000 by 2000 pixels, the confidence was 0.25, the IOU threshold was 0.2 and the model was trained for 250 epochs. The ASA detector model had a P value of 0.83, R value of 0.81, a mAP_0.5 value of 0.86 and a box loss of 0.035, while for the $CaHPO_4$ detector, these values were 0.69, 0.69, 0.70 and 0.044 respectively. The cross-entropy loss was 0 for both models, because they were each trained for a single class, therefore no classification task was feasible. The publicly accessible, pre-trained YOLOv5 model was modified during training, and as a result, the weight values for the new models were obtained. These were used for the real-time experiments.

2.2.4. Image-based API concentration calculation

For the real-time determination of the API concentration, the text files, containing the relative coordinates of the predicted bounding boxes, generated by the trained YOLOv5 model were used. These were analysed in MATLAB 9.12.0.1975300 (Mathworks, Natick, MA, USA) with a custom-made MATLAB algorithm. For the first step, each particle's diameter was calculated and with it the particle's volume was estimated using spherical approximation. After that, the API concentration of the blend could be calculated by dividing the combined volume of the API particles with the total volume, which was then averaged for every 10,000 consecutive particles. This was then compared against the results of the HPLC measurements with linear regression.

HPLC was used as a reference method to measure the ASA concentration of the samples. From each concentration level, 2–2 HPLC samples were prepared. 500 mg portions of the samples were measured into 100.0 mL volumetric flasks, then they were dissolved in a 60:40 mixture of acetonitrile (ACN) and phosphorus acid (200:1 water-phosphorus acid solution) in an ultrasound bath for 5 min. After that, the solution was filtered across a 0.45 μm polytetrafluorethylene syringe filter. The measurements were carried out using a reverse-phase Inertsil ODS-2 5 μm 250 × 4.6 mm HPLC column (GL Sciences, Torrance, CA, USA), while the flow rate was set to 1.5 mL/min. From each HPLC sample, 5.0–5.0 μl was injected and the concentration of ASA was determined based on the solution's ultraviolet absorption at 237 nm.

To assess the deep learning-based method's accuracy in predicting the API content of the powder blends, the root mean squared error of prediction (RMSEP) was calculated by using the following formula (Eq. (1)):

$$RMSEP = \sqrt{\frac{\sum_{i=1}^{n}\left(y_{predicted} - y_{measured}\right)^2}{n}} \quad (1)$$

where n is the number of samples, $y_{predicted}$ is the API content value obtained using the model and $y_{measured}$ is the API content measured with HPLC.

2.2.5. Determination of particle size distribution

The diameter values determined with the algorithm can be used to characterize the particle size of the components of the powder blends. The acquired distributions were compared to the ones acquired by a Malvern Mastersizer 2000 (Malvern Panalytical, Malvern, UK) laser diffraction analyser. A Malvern Scirocco 2000 feeding inlet (Malvern Panalytical, Malvern, UK) was used to feed the samples into the device. During the measurements, each sample weighed 2 g, while the dispersive air pressure was set to 1 bar.

3. Results and discussion

3.1. API concentration determination

The trained YOLOv5 models were used for the recognition of the ASA and CHP components of powder blends on images captured in real-time. The predicted bounding boxes were drawn onto the images, like it is shown on Fig. 4. A video containing particles recognized by the YOLOv5 models can be viewed in the supplementary (*Svid*).

It can be observed that both YOLOv5 models could successfully recognize the given types of components, without mix-ups. Furthermore, the bounding boxes are seemingly precise in bordering the particles, which is a critical factor, considering that the calculations are based on their coordinates. However it should be considered that minuscule particles are not recognized, so in the case of the current setup, these particles could not be examined.

In order to evaluate the accuracy of the prediction acquired with the

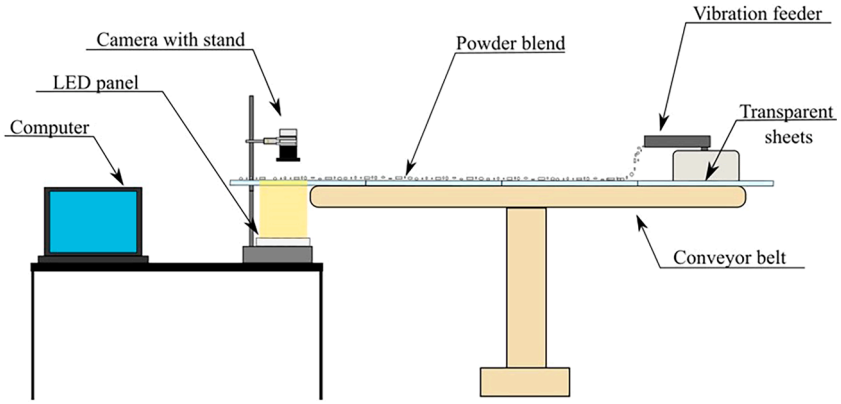

Fig. 2. Setup for the real-time imaging of the powder blends.

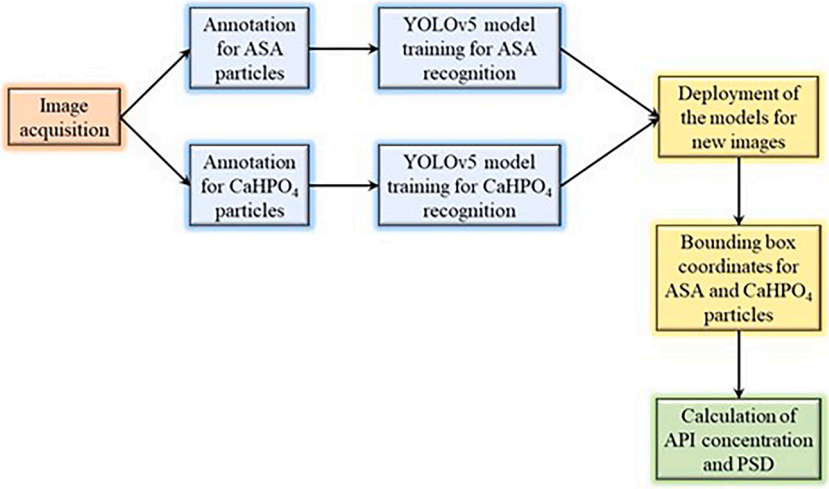

Fig. 3. A flowchart describing the training and deployment of YOLOv5 models.

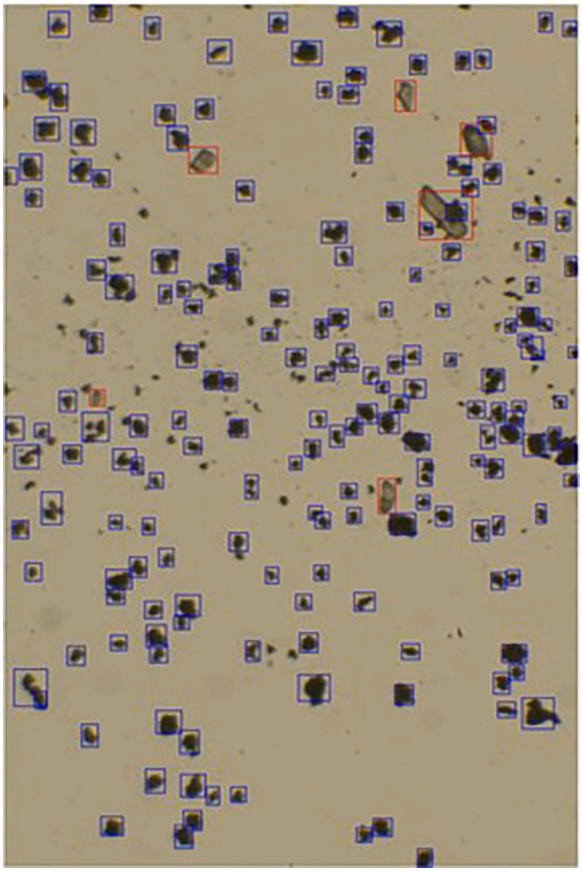

Fig. 4. Particles recognised with the YOLOv5 models. Bounding box colouring: red: ASA, blue: CHP.

YOLOv5 based method the results were compared to the HPLC measurements. Fig. 5 presents the predicted API concentration as a function of the API concentration measured by HPLC and the fitted first order polynomial.

The resulting RMSEP for the validation dataset was 0.871 m/m%. *Table 1*. shows the measured and predicted API concentrations and the relative error of the predictions for each validation level. It can be observed that the image-based method is quite accurate in determining the API concentration of the powder blends, acting as a proof of concept for the proposed system, however, there is plenty of room for improvement.

Furthermore, this method could be implemented as an on-line tool to gather accurate information on powder blends leaving batch blenders without major changes in the manufacturing line. With it, the parts of the powder blend where the API concentration is not within the prescribed range could be detected and removed, improving the content uniformity, therefore the safety of the final drug product.

3.2. *Examination of particle size distribution*

The currently used particle size analyser methods are not capable of simultaneously determining the PSD of the different components of the powder blend. If this were possible, PSD measurements would yield information of much higher quality. We discovered that the real-time, deep learning-based image analysis could provide diameter values accurate enough to compare with the results of a laser diffraction particle size analyser. Each particle's diameter value was sorted into the same particle size intervals used by the Malvern Mastersizer 2000, resulting in comparable distributions, which are presented on Fig. 6.

Comparing the distributions, it can be observed that the maxima of the curves measured by the deep learning-based system are quite close to the ones recorded with the conventional method in the case of both components, indicating the accuracy of the method. However, the resulting volume values and the width of the curves are different. The developed method did not recognize particles smaller than 100 μm, indicating that currently it only could be used on particles larger than this. At the same time, if the goal were to examine smaller particles, a different objective with higher magnification could be used providing much more accurate results for any desired size range. It should also be noted that the Malvern device uses various smoothing algorithms when creating the distribution curves, which are not exactly known to users, so it is not possible to accurately reproduce the results it produces with other methods.

The developed particle size measurement procedure has significant untapped potential. By using an objective with higher magnification or by improving the evaluation algorithm, an accuracy similar to that of laser diffraction devices could be achieved, and because of the real-time measurements, it can be used as an on-line measurement method. Unlike the currently available, dynamic image analysis particle size measurement methods, this system is capable of simultaneously determining each component's PSD in real-time, making it possible to understand the blending process's effect on the particles, thus reducing the risk of segregation during the latter production steps. Another major advantage of this method is that, apart from the final steps, its measurement setup

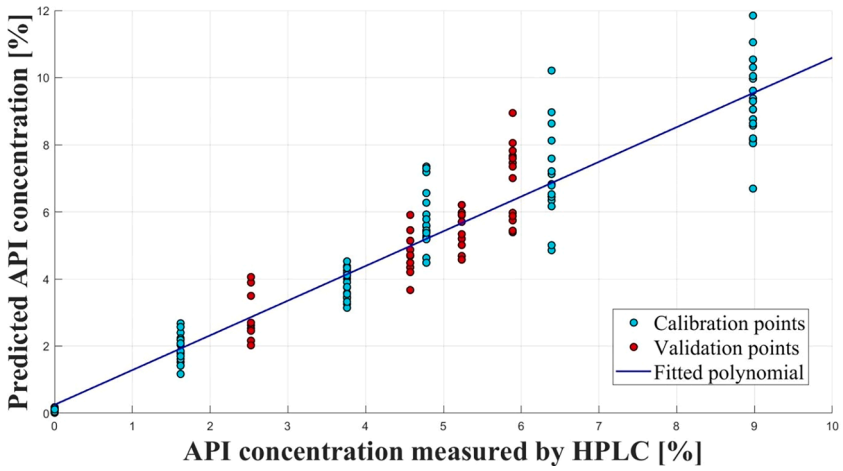

Fig. 5. The predicted API concentration of the powder blend as a function of the results measured by HPLC.

Table 1
The predicted and HPLC measured API concentrations and the relative error of the predictions for each validation level.

ASA concentration measured by HPLC[m/m%]	Average ASA concentration predicted with image analysis [m/m %]	Relative error [%]
2.525	2.882	14.15
4.573	4.812	5.22
5.235	5.441	3.93
5.890	6.947	17.95

and the processing of the acquired images is completely identical to the one suitable for the API concentration measurement, making it possible to obtain two types of key information about powder blends simultaneously in real-time. The application of these methods could significantly contribute to the improvement of the quality of the manufactured product, resulting in safer drug products for patients.

4. Conclusions

This paper presented a novel PAT system, where deep learning was combined with machine vision to determine the API concentration and the per component PSD of powder blends in real-time. YOLOv5 models were trained to recognize the ASA and CHP particles and Matlab algorithms were used to calculate the results. We demonstrated that it is possible to accurately measure the API concentration with this method by comparing the results with the ones from HPLC analysis. Furthermore, with this system, the PSD of different components of a powder blend can be measured at the same time, making it a prominent on-line PAT tool.

The method could be used for other API and excipient combinations, and even for blends with more than two components, making it possible to study the interactions between different excipients as well. By monitoring the discharged blend's API concentration, the content uniformity of the final drug product could be enhanced. If, in addition, the PSD of the powder mixture is also measured, the pharmaceutical blending process could be better understood and the manufacturing of defective product could be further reduced. In addition, this system could be implemented as an on-line tool for the monitoring of continuous blending.

CRediT authorship contribution statement

Máté Ficzere: Investigation, Methodology, Data curation, Visualization, Writing – original draft. **Orsolya Péterfi:** Investigation. **Attila Farkas:** Writing – review & editing. **Zsombor Kristóf Nagy:** Supervision, Conceptualization, Writing – review & editing. **Dorián László Galata:** Investigation, Conceptualization, Methodology, Writing – review & editing.

Declaration of competing interest

The authors declare that they have no conflicts of interest.

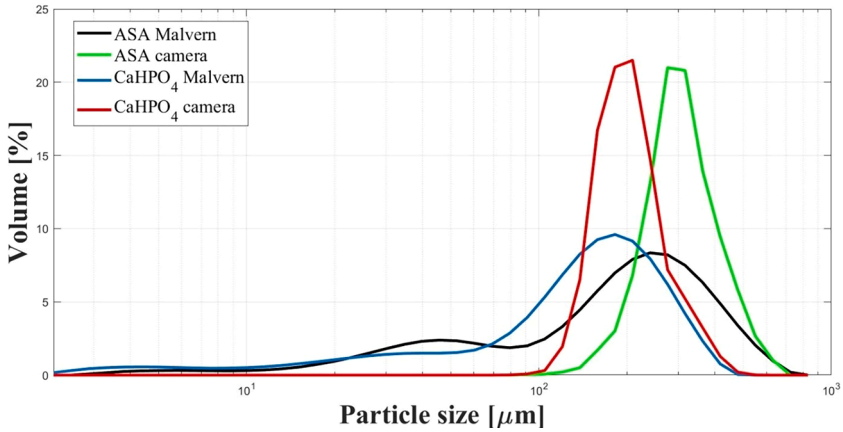

Fig. 6. Particle size distributions measured by image analysis and the Malvern Mastersizer 2000 laser diffraction particle size analyser.

Data availability

Data will be made available on request.

Acknowledgments

The research has been implemented with the support provided by the Ministry of Innovation and Technology of Hungary from the National Research, Development and Innovation Fund, financed under the [FK-132133] funding scheme. Project no. TKP-9-8/PALY-2021 has been implemented with the support provided by the Ministry of Culture and Innovation of Hungary from the National Research, Development and Innovation Fund, financed under the TKP2021-EGA funding scheme. This project was supported by the ÚNKP-23-3-I-BME-23 New National Excellence Program of the Ministry of Human Capacities. The project supported by the Doctoral Excellence Fellowship Programme (DCEP) is funded by the National Research Development and Innovation Fund of the Ministry of Culture and Innovation and the Budapest University of Technology and Economics, under a grant agreement with the National Research, Development and Innovation Office.

Supplementary materials

Supplementary material associated with this article can be found, in the online version, at doi:10.1016/j.ejps.2023.106611.

References

Berman, J., Schoeneman, A., Shelton, J.T., 1996. Unit dose sampling: a tale of two thieves. Drug Dev. Ind. Pharm. 22, 1121–1132.
Cullen, P.J., Romañach, R.J., Abatzoglou, N., Rielly, C.D., 2015. Pharmaceutical Blending and Mixing. John Wiley & Sons.
Esbensen, K.H., Román-Ospino, A.D., Sanchez, A., Romañach, R.J., 2016. Adequacy and verifiability of pharmaceutical mixtures and dose units by variographic analysis (Theory of Sampling)—a call for a regulatory paradigm shift. Int. J. Pharm. 499, 156–174.
Ficzere, M., Mészáros, L.A., Kállai-Szabó, N., Kovács, A., Antal, I., Nagy, Z.K., Galata, D. L., 2022. Real-time coating thickness measurement and defect recognition of film coated tablets with machine vision and deep learning. Int. J. Pharm. 623, 121957.
Ultralytics, 2023. https://github.com/ultralytics/yolov5.
Food, Administration, D., 2004. Guidance for industry, PAT-A framework for innovative pharmaceutical development, manufacturing and quality assurance.
Galata, D.L., Meszaros, L.A., Ficzere, M., Vass, P., Nagy, B., Szabo, E., Domokos, A., Farkas, A., Csontos, I., Marosi, G., 2021a. Continuous blending monitored and feedback controlled by machine vision-based PAT tool. J. Pharm. Biomed. Anal. 196, 113902.
Galata, D.L., Meszaros, L.A., Kallai-Szabo, N., Szabó, E., Pataki, H., Marosi, G., Nagy, Z. K., 2021b. Applications of machine vision in pharmaceutical technology: a review. Eur. J. Pharm. Sci. 159, 105717.
Garcia, T., Bergum, J., Prescott, J., Tejwani, R., Parks, T., Clark, J., Brown, W., Muzzio, F., Patel, S., Hoiberg, C., 2015. Recommendations for the assessment of blend and content uniformity: modifications to withdrawn FDA draft stratified sampling guidance. J. Pharm. Innov. 10, 76–83.
Gosselin, R., Durão, P., Abatzoglou, N., Guay, J.M., 2017. Monitoring the concentration of flowing pharmaceutical powders in a tableting feed frame. Pharm. Dev. Technol. 22, 699–705.
Hirschberg, C., Edinger, M., Holmfred, E., Rantanen, J., Boetker, J., 2020. Image-based artificial intelligence methods for product control of tablet coating quality. Pharmaceutics 12, 877.
Iwata, H., Hayashi, Y., Hasegawa, A., Terayama, K., Okuno, Y., 2022. Classification of scanning electron microscope images of pharmaceutical excipients using deep convolutional neural networks with transfer learning. Int. J. Pharm. X 4, 100135.
Jakubowska, E., Ciepluch, N., 2021. Blend segregation in tablets manufacturing and its effect on drug content uniformity—a review. Pharmaceutics 13, 1909.
Lee, S.H., Lee, J.H., Cho, S., Do, S.H., Woo, Y.A., 2012. End point determination of blending process for trimebutine tablets using principle component analysis (PCA) and partial least squares (PLS) regression. Arch. Pharm. Res. 35, 1599–1607.
Li, L., Doroslovački, M., Loew, M.H., 2020. Approximating the gradient of cross-entropy loss function. IEEE Access 8, 111626–111635.
Ma, X., Kittikunakorn, N., Sorman, B., Xi, H., Chen, A., Marsh, M., Mongeau, A., Piché, N., Williams III, R.O., Skomski, D., 2020. Application of deep learning convolutional neural networks for internal tablet defect detection: high accuracy, throughput, and adaptability. J. Pharm. Sci. 109, 1547–1557.
Madarász, L., Nagy, Z.K., Hoffer, I., Szabó, B., Csontos, I., Pataki, H., Démuth, B., Szabó, B., Csorba, K., Marosi, G., 2018. Real-time feedback control of twin-screw wet granulation based on image analysis. Int. J. Pharm. 547, 360–367.
Muthudoss, P., Kumar, S., Ann, E.Y.C., Young, K.J., Chi, R.L.R., Allada, R., Jayagopal, B., Dubala, A., Babla, I.B., Das, S., 2022. Topologically directed confocal Raman imaging (TD-CRI): advanced Raman imaging towards compositional and micromeritic profiling of a commercial tablet components. J. Pharm. Biomed. Anal. 210, 114581.
Nagy, B., Farkas, A., Borbás, E., Vass, P., Nagy, Z.K., Marosi, G., 2019. Raman spectroscopy for process analytical technologies of pharmaceutical secondary manufacturing. AAPS PharmSciTech 20, 1–16.
Padilla, R., Netto, S.L., Da Silva, E.A., 2020. In: A Survey on Performance Metrics for Object-Detection Algorithms, 2020 International Conference on Systems, Signals and Image Processing (IWSSIP). IEEE, pp. 237–242.
Razuc, M., Grafia, A., Gallo, L., Ramírez-Rigo, M.V., Romañach, R., 2019. Near-infrared spectroscopic applications in pharmaceutical particle technology. Drug Dev. Ind. Pharm. 45, 1565–1589.
Rezatofighi, H., Tsoi, N., Gwak, J., Sadeghian, A., Reid, I., Savarese, S., 2019. Generalized intersection over union: a metric and a loss for bounding box regression. In: Proceedings of the IEEE/CVF Conference on Computer Vision and Pattern Recognition, pp. 658–666.
Romañach, R.J., 2015. Sampling and determination of adequacy of mixing. Pharm. Blending Mix. 57–78.
Sachs, S., Ratz, M., Mäder, P., König, J., Cierpka, C., 2023. Particle detection and size recognition based on defocused particle images: a comparison of a deterministic algorithm and a deep neural network. Exp. Fluids 64, 21.
Sánchez-Paternina, A., Sierra-Vega, N.O., Cárdenas, V., Méndez, R., Esbensen, K.H., Romañach, R.J., 2019. Variographic analysis: a new methodology for quality assurance of pharmaceutical blending processes. Comput. Chem. Eng. 124, 109–123.
Saravanan, D., Muthudoss, P., Khullar, P., Venis, A.R., 2021. Quantitative microscopy: particle size/shape characterization, addressing common errors using 'analytics continuum'approach. J. Pharm. Sci. 110, 833–849.
Shekunov, B.Y., Chattopadhyay, P., Tong, H.H., Chow, A.H., 2007. Particle size analysis in pharmaceutics: principles, methods and applications. Pharm. Res. 24, 203–227.
Sierra-Vega, N.O., Román-Ospino, A., Scicolone, J., Muzzio, F.J., Romañach, R.J., Méndez, R., 2019. Assessment of blend uniformity in a continuous tablet manufacturing process. Int. J. Pharm. 560, 322–333.